Metrol. Meas. Syst., Vol. 25 (2018) No. 4, pp. 755–767.

PAN POLSKA AKADEMIA NAUK

METROLOGY AND MEASUREMENT SYSTEMS

Index 330930, ISSN 0860-8229

www.metrology.pg.gda.pl

M&MS

THE EFFECT OF PATTERNS ON IMAGE-BASED MODELLING OF TEXTURE-LESS OBJECTS

Jahanzeb Hafeez[1)], Hyoung-Joon Jeon[1)], Alaric Hamacher[1, 2)], Soon-Chul Kwon[1)], Seung-Hyun Lee[1)]

1) *Kwangwoon University, Department of Plasma-Bio Display, 20 Kwangwoon-ro, Nowon-gu, Seoul 01897, South Korea* (*jahanzeb@kw.ac.kr, fotojoon@kw.ac.kr, stereo3d@kw.ac.kr, ksc0226@kw.ac.kr,* ✉ *shlee@kw.ac.kr,* +82 2 940 5230)

2) *Gachon University, Department of Computer Science, 1342 Seongnamdaero, Sujeong-gu, Seongnam-si, Gyeonggi-do 13120, South Korea*

Abstract

The task of generating fast and accurate three-dimensional (3D) models of objects or scenes through a sequence of non-calibrated images is an active field of research. The recent development in algorithm optimization has resulted in many automatic solutions that can provide an accurate 3D model from texture-full objects. Structure-from-motion (SfM) is an image-based method that uses discriminative point-based feature identifier, such as SIFT, to locate feature points in the images. This method faces difficulties when presented with the objects made of homogenous or texture-less surfaces. To reconstruct such surfaces a well-known technique is to apply an artificial variety by covering the surface with a random texture pattern prior to the image capturing process. In this work, we designed three series of image patterns which are tested based on the contrast and density ratio which increases from the first to the last pattern within the same series. The performance of the patterns is evaluated by reconstructing the surface of a texture-less object and comparing it with the true data. Using the best-found patterns from the experiments, a 3D model of a Moai statue is reconstructed. The experimental results demonstrate that the density and structure of a pattern highly affects the quality of the reconstruction.

Keywords: structure-from-motion, feature detection, patterns analysis, 3D reconstruction, surface comparison.

1. Introduction

The geometric acquisition of natural and man-made objects through non-contact measuring techniques are classified into triangulation, *Time-of-Flight* (ToF), and interferometry [1]. *Structure-from-motion* (SfM) coupled with *multi-view stereo* (MVS) techniques are the state-of-the-art techniques among triangulation techniques in which 3D coordinates of the objects are measured from a collection of overlapping 2D images. A typical reconstruction procedure in SfM consists of three main steps. In the first step, camera orientation parameters (intrinsic and extrinsic) have to be determined from all images using the collinearity equations (also known as a self-calibration method). In the second step, feature points have to be identified in a sequence

Article history: received on Feb. 13, 2018; accepted on Aug. 14, 2018; available online on Dec. 31, 2018, DOI: 10.24425/mms.2018.124883.

of images and are saved into feature descriptors. Thirdly, based on the collinearity equations and with the help of feature points the 3D coordinates of the objects are estimated in a 3D space. As in SfM, MVS matching techniques use these coordinates to retrieve a dense point cloud of an object. To identify the feature points in a sequence of images, SfM uses discriminative point-based features, such as *Scale Invariant Feature Transform* (SIFT) [2] which works well to recognize the texture-rich objects with a plenty of natural or artificial elements on the surface [3, 4]. Hence, the SfM and MVS pipeline works well with surfaces that contain strong morphological features together with high frequency colour changes.

However, these methods fail when presented with objects that have little or no texture. The problem is that – to work – the point feature detector needs some distinct features on the surface.

If the surface of a processed object is texture-less, it results in incomplete and inaccurate 3D model clouds which cause serious troubles in a further reconstruction procedure. In order to solve this problem, several methods including structured light or coded patterns have been proposed. In this method, a predefined pattern is projected on the surface of a texture-less object using a calibrated projector-camera pair. If the surface of the object under observation is plane, the pattern shown in the corresponding image will be similar to that of the projected pattern. In other words, if the surface has variations in its 3D geometry, the pattern shown in the image will be distorted because of the surface geometry [5]. By using the information extracted from distortion of the pattern, the 3D geometry of the surface is estimated. This method can provide a 3D model of an object with a height error within millimetres [6, 7].

Similarly, random patterns have also been shown working well with objects made of homogeneous and texture-less surfaces [8]. In this technique a texture-less object is enriched with artificial texture by projecting a pattern onto it and taking pictures from multiple viewpoints. The projected patterns can be designed by symmetrically or randomly arranging the markers used to create them. A pattern can highly affect the quality of produced data based on its characteristics that may include shape, size, colour, and arrangement of the markers.

In this paper, we present an idea of reconstructing 3D models of the texture-less objects using image patterns. We projected artificial texture on a surface by using patterns that carry a variety of shapes. Three series of image patterns with different shapes (markers) and sizes were designed. Each series contains five patterns which are generated by arranging the markers in a way that each one has different contrast and density values. We evaluated the performance of the patterns on the basis of metrics that help the point-based features, such as SIFT, to find distinct feature points in adjacent images. As the SIFT algorithm tries to find corners and blobs in an image that are invariant to the scale and rotation of other images, artificial texture patterns with increasing density should find more feature points and subsequently provide a complete and accurate final 3D model.

2. Related work

The completeness and accuracy of a 3D model depend on the amount of feature points extracted from the captured set of images. If a surface being captured is texture rich, the quality of the produced data would be higher in comparison with poorly textured surfaces. Most of the studies dedicated to address the problem of feature extraction from a texture-less surface either used a single pattern or multiple patterns; however, density and shape of the markers were not tested to evaluate their performance when applied to a texture-less surface [9–11].

One of the systems proposed by Chang *et al.* was used to monitor the deformity of a human spine to diagnose scoliosis. In this system, they used multiple amateur cameras and projectors

to obtain a sequence of images from arbitrarily chosen viewpoints. The projectors were used to provide artificial elements by projecting a pattern onto the torso because its surface is relatively homogeneous and texture-less. The image pattern for projection was designed by randomly arranging eleven unique three-by-three sub-blocks of pixels that do not repeat within a six-pixel radius. The tests performed to measure the accuracy of the reconstructed surface yielded the RMS error (also called standard deviation) of 0.52 mm and 0.58 mm for an instantaneous and a periodic test, respectively [12].

Similarly, Popielski *et al.* designed a structured pattern to exploit the performance of different feature point detectors from a convergent pair of pictures captured from a homogeneous surface. The images were taken from the projection of a designed pattern and processed by four methods including the Harris corner detector [13], Nobel's version of auto-correlation, the Kanade-Tomasi [14], and Loy-Zelinsky [15] algorithms to extract the feature points. The extracted feature points were further processed to examine the performance of algorithms in real 3D reconstruction conditions and next they were filtered to assess the putative and filtered matches. The maximum efficiency values achieved for different algorithms were reported to be 1% for Harris, 16% for Noble, 25% for Kanade-Tomasi, and 34% for Loy-Zelinsky feature detectors, respectively [8].

Recently, Ahmadabadian *et al*. employed a low-cost system for 3D reconstruction of small and texture-less objects. The system consisted of a rotation table, one digital camera, and eight simple dot laser pointers of red and green colours. The dot laser points were placed at discrete angles to project an artificial variety of two-colour texture on the surface being captured. The experimental results showed the performance of the system approximately 10 times less when compared with the ground truth data. They concluded that a random pattern projection system that can provide a pattern of strong contrast coupled with high frequency colour changes could enhance the efficiency of their system significantly [16].

Similarly, in our previous research, we reported that with the help of random patterns one can generate 3D models of a texture-less object with a high precision of only sub-millimetre mean error. We also found that the accuracy of the final 3D model can vary based on the markers such as checkerboard, noise, squares, and tiled lines used in a pattern. From experiments, we concluded that the tiled lines was the best pattern in our experimental setup [17, 18].

Since projecting a pattern provides artificial elements on the surface of a texture-less object and helps the feature detectors to find more feature points across a sequence of images, we assume that a dense mesh of artificial features on the projection will increase the number of tie-points in adjacent images and consequently result in a complete and accurate 3D model. In this study, we want to emphasize the factors that may impact the feature extraction process by varying the density of different types of patterns.

3. 3D reconstruction and evaluation of texture-less surface

In this section we briefly describe the patterns used to collect image data followed by detailed analysis of the experiments and the obtained results.

3.1. Generation of patterns

A pattern consists of elements that – when being projected – provide an artificial variety by covering the surface of an interesting object before an image acquisition process. These elements help the feature detectors, such as SIFT, to find distinct feature points in a sequence of images. In the present study, we designed three series of patterns, namely grid, cross, and square ones. Each

series contains five patterns made of 2-bit binary images with a resolution of 1280×720 pixels. The elements in a pattern vary, specifically, in terms of shape, size, distance, black-white contrast and density ratio from the first to the last pattern within a series, as illustrated in Fig. 1. The patterns in grid and cross series were designed in GIMP while the patterns in the square series were generated using *ImageMagick* (IM). GIMP is a GNU image manipulation program [19] which provides a *graphical user interface* (GUI) while IM [20] is a command-line-based image editor which can create images dynamically and automatically. Both tools are open sourced and available for use free of charge.

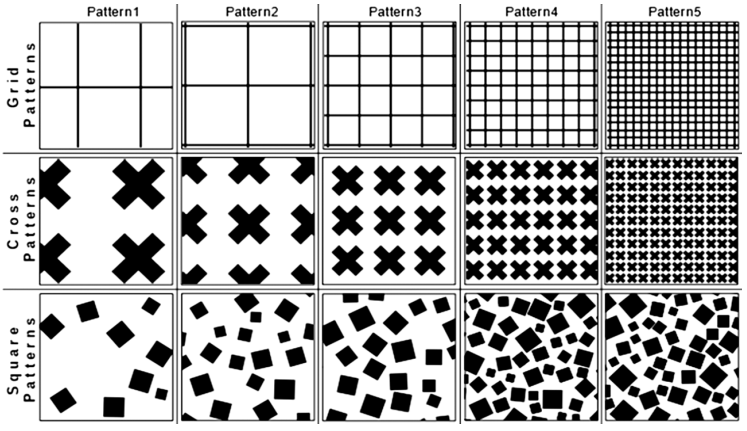

Fig. 1. Series of the grid, cross, and square patterns. Patterns are cropped to 10% of the original size of the images.

As mentioned before, every series contains five patterns and – for the purpose of this paper – the patterns in each series are called Pattern1, Pattern2, Pattern3, Pattern4, and Pattern5, respectively, as shown in Fig. 1. The patterns in grid series were designed in a way that they have repetitive structure. Although the structure of the patterns is not random, their density increases from the first to the last pattern. Similarly to the grid series, the patterns in the cross series are repetitive and their density increases from the first to the last pattern but the shape of the markers is like 'X' symbol which is supposed to provide the maximum number of edges and corner points when projected on a surface. The third series of patterns is made of random squares generated in IM using a script written in the bash language. In this series, every pattern consists of a different number of squares that are randomly placed, rotated and resized in a range between 10 to 20 pixels.

We characterized the patterns based on the contrast and minimum structural resolution of the pattern images, as shown in Table 1. In this table, contrast values represent the black pixels on

Table 1. Contrast ratio (black colour percentage) and density (minimum structural resolution) values for the series of grid, cross, and square patterns.

Pattern Series	**Pattern1**		**Pattern2**		**Pattern3**		**Pattern4**		**Pattern5**	
	Contrast [%]	Density [pixels]	Contrast [%]	Density [pixels]	Contrast [%]	Density [pixels]	Contrast [%]	Density [pixels]	Contrast [%]	Density [pixels]
Grid	3.5	114	6	96	12	48	24	24	44	12
Cross	22	93	24	65	36	43	45	26	52	9
Square	11	82	23	74	29	56	38	27	49	7

a white background in the pattern images while density is the minimum structural resolution of the patterns calculated in pixels. Moreover, the structural resolution (S_R) is calculated by taking the first deviation of a pattern image and then finding the minimum distance between pixels in adjacent lines represented as a_i and b_i in (1), where n is the total number of distances:

$$S_R = \min \sum_{i=1}^{n} \frac{a_i b_i}{n} . \tag{1}$$

Further, in this paper the terms density and structural resolution are used interchangeably and the patterns with a low structural resolution have higher density values depending on the structure of the pattern images.

3.2. Data collection and experiments

The experiments were performed by reconstructing the surface of a one-colour (black) cardboard cube. All the surfaces of the cube are plain and have no variations. A black cardboard cube is the worst-case scenario since its surface properties are very challenging for conventional SfM and MVS pipeline. To reduce the time-consuming proceedings, only one surface (top) of the cube was considered to be imaged. The image data were acquired using a *multi-camera rig system* (MCRS) previously developed by the same authors, as reported in [17, 21].

An MCRS comes with a number of advantages in the field of 3D reconstruction, since it provides the operators with a controlled and constant environment, especially when multiple image datasets either from a single object or multiple objects are needed to be collected. On the other hand, most of the 3D reconstruction procedures are easy to use for non-professionals but capturing suitable images makes the process time-consuming and difficult for an inexperienced operator. In that case the MCRSs are helpful to capture a large number of small complex objects – such as museum objects – for 3D reconstruction.

By using the MCRS, a total of 15 pattern-based sequences of image data were captured. Each sequence contained 10 images of the cardboard cube's top surface taken from arbitrarily chosen positions while being enriched by the image patterns that were always projected from the same static position. The illumination condition, exposure time, camera positions and orientations were identical for all sets of images, as illustrated in Fig. 2. To investigate the efficiency of the feature point identification, the cardboard cube was also captured in regular daylight without projecting a pattern.

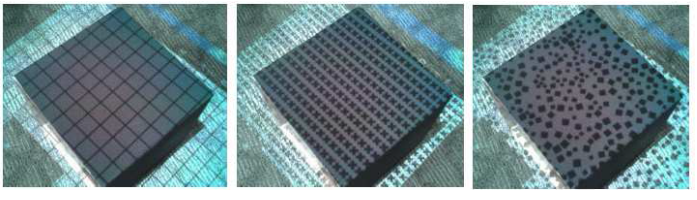

Fig. 2. A cardboard cube under the projection of grid (left), cross (centre), and square (right) patterns.

Having completed the image acquisition process, all sequences of image data were processed by SfM-MVS pipeline using freeware software VisualSfM (VSfM) and MeshLab. VSfM is an academic tool and it offers a complete SfM-MVS algorithm pipeline [22, 23]. It takes images as input, processes them in three steps including (1) feature point extraction and their matching,

(2) sparse reconstruction, and (3) dense reconstruction of the point clouds. More specifically, the 3D reconstruction process is started by initiating the automated calibration of camera parameters followed by alignment of the images and reconstruction of the point clouds.

According to Remondino *et al.*, the 3D data obtained from the automated camera calibration was found to be reliable for the software which is used in our work [24]. Thus, the camera calibration was achieved solely by the software. For the image data obtained with no pattern, the first step in the SfM proceedings failed to identify the feature points from the images due to lack of features on the cube's surface. Furthermore, the sequences of image data obtained under the projection of designed patterns were processed using the SfM-MVS pipeline and a dense 3D reconstruction of the point clouds was obtained. Table 2 shows the number of points found for each corresponding pattern in the resulted point clouds. We observed that with an increase in density of the patterns, a higher number of points was detected in the point clouds. This indicates that there is a subsequent increase in the detected feature points when density of the patterns is increased, what consequently results in a complete and dense 3D surface reconstruction of the object.

Table 2. Numbers of points found in the point clouds for the series of grid, cross and square patterns.

Pattern Name	Grid Patterns	Cross Patterns	Square Patterns
Pattern1	105,266	107,356	105,570
Pattern2	109,633	114,326	110,019
Pattern3	119,211	113,236	112,337
Pattern4	129,513	117,852	110,683
Pattern5	134,499	123,527	115,092

3.3. Comparison and evaluation

We have evaluated the 3D models reconstructed with images in relation to the reference models in terms of surface deviation. Our comparison pipelines included the open-sourced and freely available Meshlab and CloudCompare software [26]. Meshlab was used to create the reference models to compare with the image-based 3D models described in Subsection 3.2. Since the surface of the generated models was plane and had no variations, a plane or a grid was considered to be the reference data. On the other hand, CloudCompare was used to calculate the surface deviation between the image-based models and reference models. The 3D point clouds generated by VisualSfM were given in arbitrary units, therefore no standard unit is defined.

Before comparing the surface models reconstructed from images with the true data (reference models), the unnecessary background points were removed using the segmentation tool in CloudCompare as it is useful to avoid disturbances during the alignment procedure. At this stage, a plane being the ideal surface was created in MeshLab. Since some of the point clouds were denser than others, we created a reference model for each generated model and the number of vertices in the reference models was considered to be equal to that in the respective point clouds.

To show the real accuracy of the generated models, point-to-point comparison is a good method. In this method, the generated models were precisely registered with the reference models using the *iterative closest point* (ICP) registration [25] and the differences between points on the surface of reconstructed models and points on the reference models were calculated. As a result

of the differences between points on both surfaces, the standard deviation σ of the square of signed distances d_i was calculated to express the variations between both surfaces. The standard deviation is defined as:

$$\sigma = \sqrt{\frac{1}{n-1}\sum_{i=1}^{n}\left(d_i - \overline{d}\right)^2}, \tag{2}$$

where n is the number of points.

Furthermore, the plane fitting method was used to assess the planarity and level of noise on the surface of generated models. The criterion defined for this method is the *root mean square error* (RMSE) of the distances between points on the surface of generated models to the best-fit plane placed at an average distance of zero.

Figure 3 illustrates the results of point-to-point comparison of 3D models generated with images captured from the projections of grid, cross, and square patterns, respectively. It expresses a heat-map representation of the signed distances in which the red colour represents the situation where the surface of generated models is above the reference models, whereas the blue colour – where it is under the reference models. In this figure, it is clear that the majority of points on the surface of generated models are closer to the points on the surface of reference models. It is also shown in Table 3.

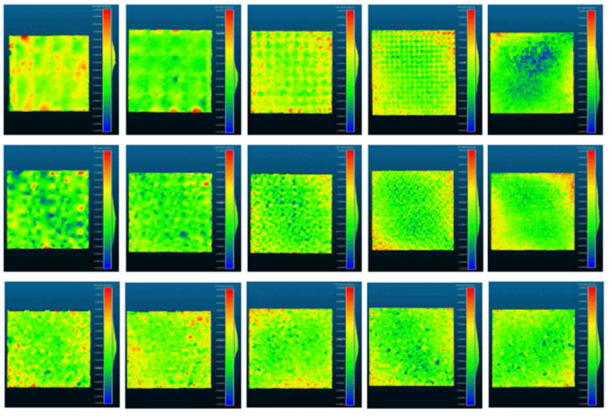

Fig. 3. A heat-map representation of the distances between the generated and reference models for the series of grid (top row), cross (centre row), and square patterns (last row).

Table 3. The mean distance and standard deviation of the distances between points on the surface of generated models and those on the reference models.

Pattern Series	**Pattern1**		**Pattern2**		**Pattern3**		**Pattern4**		**Pattern5**	
	M.D	S.D	M.D	S.D	M.D	S.D	M.D	S.D	M.D	S.D
Grid	1.9×10^{-4}	2.1×10^{-3}	1.7×10^{-4}	2.2×10^{-3}	0.1×10^{-4}	0.9×10^{-3}	0.2×10^{-4}	1.3×10^{-3}	0.8×10^{-5}	1.0×10^{-3}
Cross	0.7×10^{-4}	1.6×10^{-3}	1.2×10^{-4}	1.9×10^{-3}	0.4×10^{-5}	1.0×10^{-3}	1.2×10^{-4}	0.8×10^{-3}	0.5×10^{-5}	0.6×10^{-3}
Square	0.2×10^{-4}	1.2×10^{-3}	-0.2×10^{-4}	0.9×10^{-3}	0.1×10^{-4}	0.9×10^{-3}	0.1×10^{-4}	1.2×10^{-3}	0.4×10^{-5}	0.7×10^{-3}

Table 4 indicates the RMSE criterion defined for the plane fitting test. The plane fitting test also revealed similar results to those of the point-to-point comparison. The lower values for RMSE show that the level of noise is far less in the point clouds generated with higher density

patterns than that generated with lower density patterns. Also, the patterns with higher density gave the more plane surface models.

Table 4. Standard deviation of the distances obtained with the plane fitting method.

Pattern Series	Pattern1	Pattern2	Pattern3	Pattern4	Pattern5
Grids	2.5×10^{-3}	2.5×10^{-3}	0.7×10^{-3}	1×10^{-3}	0.9×10^{-3}
Crosses	1.6×10^{-3}	1.7×10^{-3}	1.0×10^{-3}	0.7×10^{-3}	0.6×10^{-3}
Squares	0.8×10^{-3}	0.7×10^{-3}	0.7×10^{-3}	1×10^{-3}	0.7×10^{-3}

For better understanding and comparative measurements of the results, graphs of the pattern density, number of points and standard deviation calculated for each generated model are plotted in Fig. 4. Fig. 4a illustrates that with an increase in contrast of the grid patterns, the number of points found in the corresponding point clouds increases gradually. The change (increment) in the number of points is clearly visible from the first to the last pattern, while this trend is not the same for the other two series of cross and square patterns. For the series of cross patterns, with an increase in contrast of the patterns, the number of points also increases but the observed difference is smaller than for the first series. In the case of square patterns, the numbers of points found in the point clouds are random. From the graph, it is evident that the patterns in the grid series are able to find a higher number of points in the point clouds in comparison with the other series.

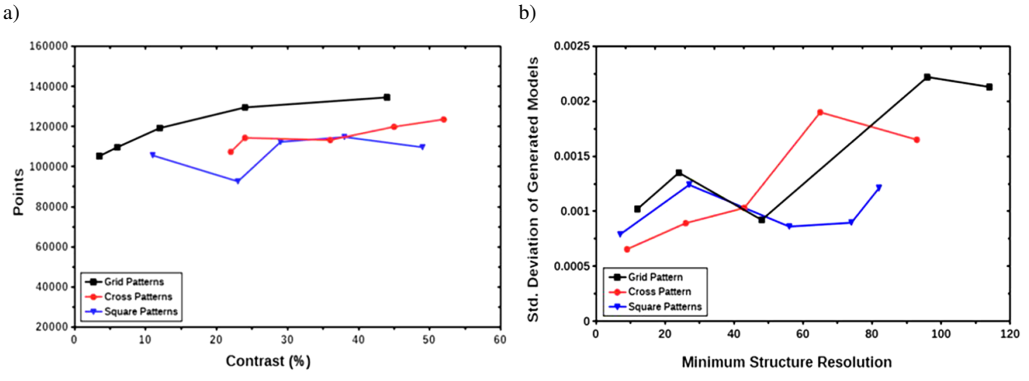

Fig. 4. Comparative results for the patterns in grid, cross, and square series. a) The co-relation between contrast and number of points found in the point clouds. b) The co-relation between minimum structure resolution and standard deviation of the distances between the generated and reference models.

Figure 4b illustrates the real accuracy of the patterns based on the point-to-point comparison. A lower value for this test indicates the capability of the patterns to be used in 3D reconstruction of complex objects. In this figure it can be seen that the models generated with patterns having the minimum structural resolution, exhibit lower deviations towards the ground truth. As indicated in Table 3, Pattern5 in the cross series exhibits minimum deviations towards the ground truth, followed by Pattern5 in the square series. Here it is worth mentioning that these two patterns have the highest contrast and density among the designed series of patterns. The evaluation results of the cube's surface indicate that patterns in each series have different effects on the achieved

reconstruction quality. This leads to establishing an objective conclusion that each series has a different impact on the 3D reconstruction of a texture-less surface.

When generating 3D models of texture-less surfaces using other projection techniques including laser triangulation and structured light, occlusions and projection focus are the main issues. Nevertheless, the image data acquisition process in traditional image-based techniques may overcome these issues by capturing the images from multiple viewpoints. Moreover, the quality of reconstruction also depends on the surface topography. As in our case, the surface of the reconstructed object is black coloured that absorbs light and therefore results in losing sharpness of the pattern depiction. Moreover, the colour aberration introduced by the projector lens is also visible on the object's surface which may produce noise on the generated models resulting in a higher surface deviation when compared with the reference data.

4. Moai (Statue) reconstruction and evaluation

To test the efficiency and robustness of the patterns we imaged a popular figure from the Easter islands, the head of Moai statue – with and without projection of patterns. The head of Moai statue was constructed using a 3D printer in one-colour (white) and a height of 160 mm. The reason why this object was selected is that most of the surfaces of Moai head are relatively flat which is appropriate for our purpose. The object was then imaged using the best performing patterns, Pattern3 from the grid, Pattern5 from the cross, and Pattern5 from the square series. The object was also imaged in regular daylight without projecting the patterns. Afterwards, the 3D models reconstructed with image data were eventually compared with the reference model acquired from the *stereolithography* (STL) file used to create it. Fig. 5 shows a schematic used to create and evaluate the 3D models of the Moai statue with patterns. In this figure, each block represents the steps involved in 3D reconstruction and evaluation of the surfaces, whereas internal elements of the blocks contain procedures needed to complete each step in a sequence.

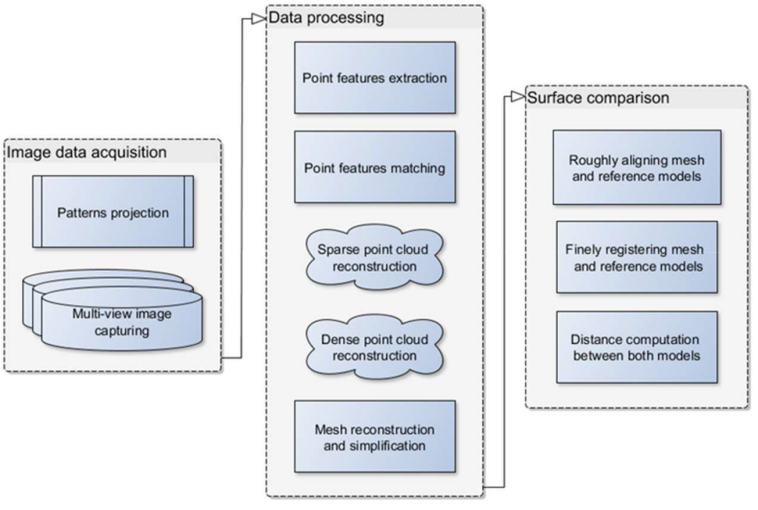

Fig. 5. A workflow scheme for the image capturing, 3D reconstruction and evaluation of a texture-less object.

Figure 6 shows the 3D models of the Moai head obtained with and without the projection of patterns. The results visually confirm that a dense pattern such as Pattern5 in the cross series

can provide an accurate and complete 3D model from a texture-less object. For comparison and evaluation, the 3D model of the Moai head generated with the projection of patterns was appropriately scaled to match the reference model. Two tests including (1) point-to-point comparison and (2) cross-sections, were performed. These methods are popular and commonly used by the researchers to assess the quality and accuracy of a final 3D model. In the first test both the image-based 3D model and the reference model were precisely registered using the ICP algorithm and the differences between points on the surface of generated model and points on the surface of reference model were calculated. As a result of the differences between points on both surfaces, we expressed the standard deviation using the *root mean square error* (RMSE), representing variations between both surfaces, as illustrated in Fig. 7a.

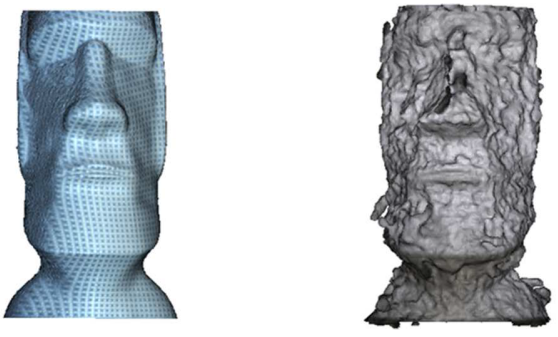

Fig. 6. The 3D models of the Moai statue generated with a pattern (left) and without a pattern (right).

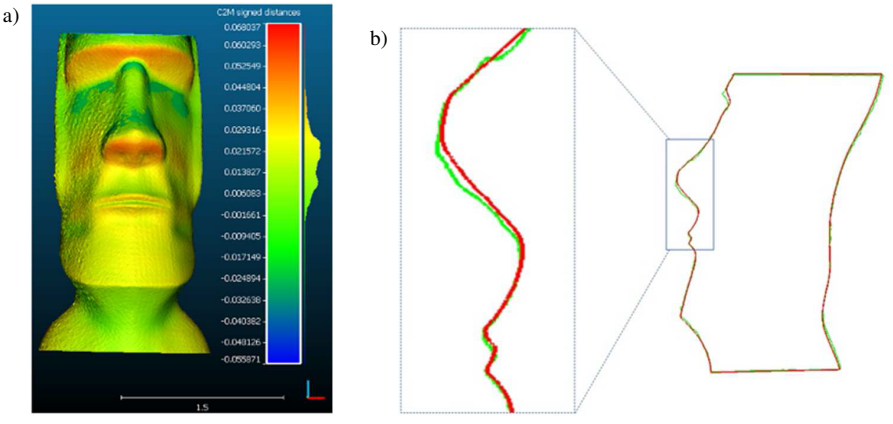

Fig. 7. Evaluation of Moai statue with the methods of: a) point-to-point comparison and b) cross-sections.

The mean distance and the standard deviation of distances between the models generated with patterns and the reference model were calculated and are shown in Table 5. From Table 3, Table 4 and Table 5, it is clear that Pattern5 from the cross series exhibits minimum deviations in both scenarios – the first scenario was the pattern-based 3D reconstruction of a plane surface while in the second scenario the whole surface with variations in its geometry was reconstructed. It leads to a conclusion that Pattern5 from the cross series performed well and provided the most accurate surface models in terms of surface deviation.

Table 5. Mean distance and standard deviation of the distances for Moai statue.

Pattern Name	Mean Distance [mm]	Standard Deviation [mm]
Pattern3 from Grid series	0.4	1.3
Pattern5 from Cross series	0.07	**0.9**
Pattern5 from Square series	0.2	0.9
No Pattern	−0.97	13.4

The cross-sections are useful for assessment of the structure and variations in the structure are compared. This test also brings out the level of detail of the structure geometry. In this test, both the 3D model reconstructed with Pattern5 in the cross series and the reference model were aligned and sections were extracted. Fig. 7b illustrates the results provided by the cross-sections extracted from the 3D model of the Moai statue generated with pattern (green line) – with those from the reference model (red line). This test showed that the structure geometry was well retained with a sufficient amount of details in the features. In the figure, it can be seen that some regions are slightly misaligned from the reference model. Later it was observed that the misaligned regions were covered with shadows produced by illumination of projectors during the image acquisition process which resulted in an incorrect estimation of the coordinates recovered by the SfM techniques.

5. Conclusion

In this study, we analysed the performance of the patterns in reconstructing the surface of homogeneous and texture-less objects. It has been proved that the use of artificial texture patterns improves the process of extracting feature points. Also, the structures of patterns significantly affect the quality of 3D reconstruction. We tested three series of patterns where each series exhibits distinct properties. Sequentially, with an increase in density and contrast of the patterns, higher numbers of points were found in the respective point clouds. However, this result may occur due to the randomness in the structure of patterns in the square series. Generally, patterns in the grid series enabled to find the highest number of points in the respective point clouds.

In order to show the real accuracy, we compared the generated models with the true data. Two tests were performed including point-to-point comparison and plane fitting methods. The criterion defined for these tests was the root mean square of the distances between the surface of generated models and the true data, expressed as standard deviation. As a result, Pattern5 in the cross series exhibited minimal deviations towards the reference model, followed by Pattern5 in the square series. Interestingly, we also found that the 3D models with the highest number of points were not the most accurate ones. The 3D reconstruction of Moai statue was also carried out. As a result, the standard deviations calculated for both the 3D model generated with Pattern5 in the cross series and without a pattern were equal to 0.9 mm and 13.4 mm, respectively. A large difference between the values demonstrates the efficiency and robustness of the patterns in terms of accuracy.

The testing of other feature detectors is also needed to achieve the best performance of the patterns. In the future work, the authors of this paper are motivated to examine if the algorithms like SURF and Harris corner detector have an influence on a wide range of test samples in certain conditions.

Acknowledgements

This research was supported by the MSIP (Ministry of Science, ICT and Future Planning), Korea, under the ITRC (Information Technology Research Center) support program (IITP-2016-R0992-16-1008) supervised by the IITP (Institute for Information & communications Technology Promotion) and by IITP grant funded by the Korean government (MSIP) (No.2017-0-00833).

References

[1] Remondino, F., El-Hakim, S. (2005). Critical overview of image-based 3D modeling. *Rec. Model. Vis. Cult. Herit. Proc. Int. Workshop Cent. Stefano Franscini Monte Verita Ascona Switz.*, 299.

[2] Lowe, D.G. (2004). Distinctive image features from scale-invariant keypoints. *Int. J. Comput. Vis.*, 60(2), 91–110.

[3] Fuhrmann, S., Langguth, F., Moehrle, N., Waechter, M., Goesele, M. (2015). MVE – An image-based reconstruction environment. *Comput. Graph.*, 53, 44–53.

[4] Hafeez, J., Hamacher, A., Son, H., Pardeshi, S., Lee, S. (2016). Workflow Evaluation for Optimized Image – Based 3D Model Reconstruction. *Int. Conf. Electron. Electr. Eng. Comput. Sci. EEECS Innov. Converg.*, 2, 62–65.

[5] Geng, J. (2011). Structured-light 3D surface imaging: a tutorial. *Adv. Opt. Photonics*, 3(2), 128–160.

[6] Salvi, J., Fernandez, S., Pribanic, T., Llado, X. (2010). A state of the art in structured light patterns for surface profilometry. *Pattern Recognit.*, 43(8), 2666–2680.

[7] Gupta, M., Agrawal, A., Veeraraghavan, A., Narasimhan, S.G. (2011). Structured light 3D scanning in the presence of global illumination. *Comput. Vis. Pattern Recognit. CVPR 2011 IEEE Conf.*, 713–720.

[8] Popielski, P., Wróbel, Z. (2012). *The Feature Detection on the Homogeneous Surfaces with Projected Pattern, in Information Technologies in Biomedicine.* (eds. Piętka, E., Kawa, J.). Springer Berlin Heidelberg, 118–128.

[9] Apuzzo, N. (2002). Measurement and modeling of human faces from multi images. *Int. Arch. Photogramm. REMOTE Sens. Spat. Inf. Sci.*, 34(5), 241–246.

[10] Wong, S.S., Chan, K.L. (2010). 3D object model reconstruction from image sequence based on photometric consistency in volume space. *Pattern Anal. Appl.*, 13(4), 437–450.

[11] Sansoni, G., Trebeschi, M., Docchio, F. (2006). Fast 3D profilometer based upon the projection of a single fringe pattern and absolute calibration. *Meas. Sci. Technol.*, 17(7), 1757.

[12] Detchev, I., Habib, A., Chang, Y.C. (2011). Image Matching and Surface Registration for 3D Reconstruction of a Scoliotic Torso. *Geomatica*, 65(2), 175–187.

[13] Harris, C., Stephens, M. (1988). *A Combined Corner and Edge Detector*. 23.1–23.6.

[14] Shi, J., Tomasi, C. (1994). *Good features to track*. 593–600.

[15] Loy, G., Zelinsky, A. (2002). A Fast Radial Symmetry Transform for Detecting Points of Interest. *Computer Vision – ECCV 2002*, 2350, Springer Berlin Heidelberg, 358–368.

[16] Ahmadabadian, A.H., Yazdan, R., Karami, A., Moradi, M., Ghorbani, F. (2017). Clustering and selecting vantage images in a low-cost system for 3D reconstruction of texture-less objects. *Measurement*, 99, 185–191.

[17] Hafeez, J., Kwon, S.C., Lee, S.H., Hamacher, A. (2017). 3D Surface Reconstruction of Smooth and Textureless Objects. *Int. Conf. Emerg. Trends Innov. ICT ICEI*, 145–149.

[18] Hafeez, J., Hamacher, A., Kwon, S., Lee, S. (2017). Performance evaluation of patterns for image-based 3D model reconstruction of textureless objects. *Int. Conf. 3D Immers. IC3D*, 1–5.

[19] GIMP. *https://www.gimp.org/* (2017).

[20] ImageMagick. *https://www.imagemagick.org/script/index.php* (2017).

[21] Hafeez, J., Lee, S., Kwon, S., Hamacher, A. (2017). Image Based 3D Reconstruction of Texture-less Objects for VR Contents. *Int. J. Adv. Smart Converg.*, 6(1), 9–17.

[22] Wu, C. (2013). Towards Linear-Time Incremental Structure from Motion. *Proc. 2013 Int. Conf. 3D Vis.*, 127–134.

[23] Wu, C., Agarwal, S., Curless, B., Seitz, S.M. (2011). Multicore bundle adjustment. *CVPR*, 3057–3064.

[24] Remondino, F., Pizzo, S.D., Kersten, T.P., Troisi, S. (2012). Low-Cost and Open-Source Solutions for Automated Image Orientation – A Critical Overview. *Prog. Cult. Herit. Preserv.*, 40–54.

[25] Besl, P.J., McKay, H.D. (1992). A method for registration of 3-D shapes. *IEEE Trans. Pattern Anal. Mach. Intell.*, 14(2), 239–256.

[26] CloudCompare. *http://www.cloudcompare.org/* (2018).